Acidity of dibasic carbon acids. Part 3.[1,2] Ion solvation state of monometallic salts of 9,10-dihydroanthracene and its derivatives in THF

Roy E. Hoffman, Malka Nir, Israel O. Shapiro * and Mordecai Rabinovitz *

Department of Organic Chemistry, The Hebrew University of Jerusalem, Givat Ram, Jerusalem, Israel 91904

The ion solvation state of monometallic salts of 9,10-dihydroanthracene (DHA) and its 9,10-disubstituted derivatives in THF has studied by UV–VIS and ^1H and ^{13}C NMR spectroscopy. At room temperature, lithium 9-phenyl-9,10-dihydroanthracen-9-ide, lithium 9,10-dimethyl-9,10-dihydroanthracenide and lithium 9,10-diphenyl-9,10-dihydroanthracenide exist as solvent separated ion pairs (SSIP). Lithium 9,10-dihydroanthracene, lithium 9-methyl-9,10-dihydroanthracen-10-ide and sodium, potassium and rubidium 9-phenyl-9,10-dihydroanthracen-9-ides, 9,10-dimethyl-9,10-dihydroanthracenides and 9,10-diphenyl-9,10-dihydroanthracenides exist as a mixture of SSIP and contact ion pairs (CIP). Sodium, potassium, rubidium and caesium 9,10-dihydroanthracenides, 9-methyl-9,10-dihydroanthracen-10-ides and 9-cyano-9,10-dihydroanthracenides exist as CIP in solution. The stabilizing effect of the methyl and phenyl substituents is more significant for SSIP than for CIP. The thermodynamics for SSIP to CIP conversion is determined for the sodium salts of DHA and its derivatives. $\Delta S°$ is 27 ± 2 cal mol^{-1} K^{-1} $\Delta H°$ increases with substituent size and charge dispersion. A model for the transition of CIP of alkali-metal salts of DHA and its derivatives into SSIP is suggested. The model takes into account the geometry and charge distribution in anions.

The main goal of our investigations is to explain the influence of electronic and geometric anion structure, the nature of counter-ions and temperature on the reactivities of mono- and di-anions. In this study we have concentrated on 9,10-dihydroanthracene (DHA) and its 9,10-substituted derivatives. Two factors determine the reactivity of anions in solution. One is the structure and charge distribution in the anions and the other is the cation–anion interaction in solution. In our preceding report[2] we presented the spatial and electronic structures of mono- and di-anions of DHA and their derivatives (Scheme 1). Here we present a study of the influence of the cation, anion structure and temperature on the structure of monometallic salts of DHA and its derivatives by UV–VIS and NMR spectroscopy. The structure of ion pairs of a few monolithium and monosodium salts of DHA and several of its monosubstituted derivatives in ethereal solvents have been studied by Szwarc,[3–5] Daney[6] and Rabideau.[7,8]

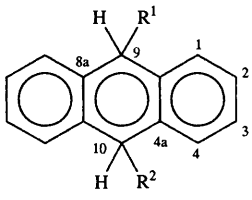

$R^1 = R^2 = H$: DHA
$R^1 = Me$; $R^2 = H$: MDHA
$R^1 = CN$; $R^2 = H$: CNDHA
$R^1 = Ph$; $R^2 = H$: PDHA
$R^1 = R^2 = Me$: DMDHA
$R^1 = R^2 = Ph$: DPDHA

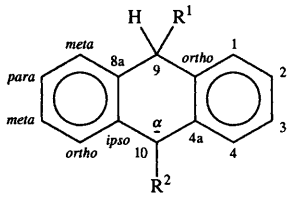

$R^1 = R^2 = H$: DHA^-
$R^1 = Me$; $R^2 = H$: $MDHA\text{-}10^-$
$R^1 = Ph$; $R^2 = H$: $PDHA\text{-}10^-$
$R^1 = R^2 = Me$: $DMDHA^-$
$R^1 = R^2 = Ph$: $DPDHA^-$

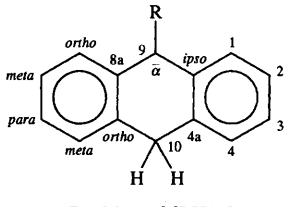

R = Me: $MDHA\text{-}9^-$
R = CN: $CNDHA\text{-}9^-$
R = Ph: $PDHA\text{-}9^-$

Scheme 1

Results and discussion

Preparation of monometallic salts

Monometallic salts were formed by reacting dimetallic salts with methanol. Dimetallic salts were prepared by exposing anthracene and its derivatives to alkali metals. The reaction proceeds according to eqn. (1), were A is anthracene, 9-

$$A \xrightarrow[THF]{M} A^{\cdot-}M^+ \xrightarrow[THF]{M} A^{2-}2M^+ \xrightarrow[-CH_3O^-M^+]{CH_3OH} AH^-M^+ \quad (1)$$

methylanthracene, 9,10-dimethylanthracene, 9-phenylanthracene, 9,10-diphenylanthracene or 9-cyanoanthracene, and M is an alkali metal.

Most of the methanol reacted with the dimetallic salt but some dianion always remained. The abbreviations used for the monometallic salts of DHA and its derivatives are given in Scheme 1. 9,10-Dimetallic salts of 9-methyl-9,10-dihydroanthracene (MDHA), 9-phenyl-9,10-dihydroanthracene (PDHA), and 9-cyano-9,10-dihydroanthracene (CNDHA) can be protonated at the 9 or 10 positions by this reaction (Scheme 1). The UV–VIS (in THF) and NMR spectra (in [$^2H_8$]THF) of the monometallic salts permit a clear structural determination. The absolute values and cation dependence of λ_{max} of monometallic salts of DHA and MDHA are practically identical (Table 1). On the other hand, the absolute values and cation dependence of λ_{max} for monometallic salts of MDHA and 9,10-dimethyl-9,10-dihydroanthracene (DMDHA) are very different. Therefore, the structures of DHA^- and $MDHA^-$ are similar but different from $DMDHA^-$ suggesting that most of the $MDHA^-$ is

Table 1 λ_{max} Of monometallic salts of DHA and its derivatives in THF at 298 K

Carbon acid	λ_{max}/nm					
	Li^+	Na^+	K^+	Rb^+	Cs^+	SSIP
DHA	400	425	442	444	446	450
MDHA	402	425	441	442	445	452
DMDHA	458	451	451	450		458
PDHA	460	449	447	443		460
DPDHA	460	448	442	443		460
CNDHA		368	380	381		

deprotonated at C-10. The monometallic salts of PDHA yield UV–VIS spectral properties more similar to the monometallic salts of 9,10-diphenyl-9,10-dihydroanthracene (DPDHA) than DHA indicating that PDHA is mostly deprotonated at C-9. The spectroscopic measurements for the monometallic salts of 9,10-dicyano-9,10-dihydroanthracene are unavailable. However, the UV–VIS spectroscopic properties of the monometallic salts $CNDHA^-$ are so different from those of DHA^- that they strongly indicate deprotonation at C-9. Additionally, λ_{max} of $CNDHA^-$ is very similar to that of the diphenylcyanomethyl anion (λ_{max} = 385 nm with counter ion Li^+ and λ_{max} = 400 nm with counter ion Cs^+ in dimethoxyethane).[9] The UV–VIS spectra of 9,9-dimethyl-9,10-dihydroanthracene (λ_{max} = 444 nm), 9,9,10-trimethyl-9,10-dihydroanthracene (λ_{max} = 452 nm) and 9,9-dimethyl-10-phenyl-9,10-dihydroanthracene (λ_{max} = 450 nm) also supported the conclusion regarding the site of the anion centre in $MDHA^-$ and $PDHA^-$.[10]

^{13}C NMR spectroscopy is consistent with the deprotonation sites suggested by the UV–VIS result.[11–13] We measured both ^1H and ^{13}C NMR spectra of the monosodium salts of MDHA, PDHA and CNDHA and found $MDHA^-$ to be 92% deprotonated at C-10, $PDHA^-$ to be 77% deprotonated at C-9 and $CNDHA^-$ to be 88% deprotonated at C-9. Previous reports had claimed 100% selectivity of deprotonation site.[11,12] In the ^1H NMR spectrum, singlets are expected only for the methyl protons of $MDHA^-$ (H-1′), H-9 and H-10. When deprotonation occurs on C-9, H-9 yields no signal and the singlet corresponding to H-10 has an integral corresponding to two protons. However, when deprotonation is on C-10, both H-9 and H-10 yield singlets, each with an integral of one proton equivalent.

Cation effect

The UV–VIS spectrum of the monolithium salt of DHA in THF displays two absorptions at 400 and 450 nm at 298 K. The absorption at 450 nm is stronger than that at 400 nm. With decreasing temperature, the absorption at 450 nm increases at the expense of the absorption at 400 nm. From these results it may be concluded that the signal at 400 nm corresponds to CIP and that at 450 nm to SSIP.[4] While Nicholls and Szwarc[4] concluded that the monolithium salt of DHA exists mainly as CIP our results clearly indicate a mixture of CIP and SSIP at 298 K.

The monosodium salt of DHA displays only one maximum over a wide range of temperatures. The wavelength, however, does change from 455 nm (228 K) to 425 nm (298 K).[4–6] This is consistent with our results (Table 1). The change in the absorption spectrum was explained as arising from the 'dynamic model' of ion pairs[14,15] by transition from SSIP (λ_{max} = 455 nm) to CIP (λ_{max} = 425 nm). According to this model, the barrier separating the SSIP and CIP states is low and the potential wells characterizing these states are shallow for anionic systems, which are large and delocalized, or with a large cation. Rising temperature changes both the shape and depth of the potential wells and the barrier height. Therefore, the structure of the ion pairs is gradually transformed from SSIP to CIP. For such salts, the UV–VIS spectrum displays only one absorption maximum. Changes in conditions shift the wavelength towards that of the more stable ion solvation state. Such behaviour has been observed not only for alkali metal salts of DHA[3,4] but also for salts of triphenylmethane.[16]

The UV–VIS, spectra of other alkali-metal salts of DHA also display only one absorption (Table 1). Going from DHA^-K^+ to DHA^-Cs^+ yields a red shift of λ_{max} but a second absorption does not appear. The absorption wavelength correlates to the cation radius according to eqn. (2) with a correlation coefficient of 0.994.

$$\lambda_{max}\,(nm) = (473.2 \pm 1.2) - (44.5 \pm 1.2)/r_+\,(nm) \quad (2)$$

As shown above, the anionic structures of the monometallic salts of DHA and MDHA are similar. Therefore, the behaviour of their absorptions with cation changes should be similar. The UV–VIS spectrum of the lithium salt of MDHA displays a peak at 452 nm with a shoulder at 402 nm (298 K). On cooling, the shoulder decreases and is therefore attributable to CIP while the peak at 452 nm corresponds to SSIP. The UV–VIS spectra of other alkali-metal salts of MDHA display only one absorption at 298 K (Table 1). $MDHA^-Na^+$ displays only one maximum that shifts from 452 nm (228 K) to 425 nm (298 K) similar to the behaviour of DHA^-Na^+. Eqn. (3) shows the correlation of the wavelength

$$\lambda_{max}\,(nm) = (469.8 \pm 1.2) - (41.0 \pm 1.2)/r_+\,(nm) \quad (3)$$

with cation radius for $MDHA^-M^+$ with a correlation coefficient of 0.997.

From these results, it follows that the monolithium salts of DHA and MDHA exist as a mixture of CIP and SSIP at room temperature but that the SSIP concentration is larger than the CIP concentration. The other monoalkali salts are mainly CIP at room temperature.

The UV–VIS spectra of monometallic salts of DMDHA, PDHA and DPDHA yield only one maximum at 298 K. In contrast with the behaviour of DHA^-M^+ and $MDHA^-M^+$, their absorptions exhibit a blue shift with increasing cation size (Table 1). Cooling solutions of monolithium salts of these compounds to 213 K does not have an effect on the absorption frequencies of their UV–VIS spectra. Therefore, we conclude that the monolithium salts of DMDHA, PDHA and DPDHA exist as SSIP in THF at 298 K. The UV–VIS absorption shifts to shorter wavelength with increasing cation size, therefore, the transition from lithium salts to sodium, potassium and rubidium salts leads to decreasing SSIP concentration.

According to our calculations,[2] the negative charge is concentrated on the deprotonated carbon atom of the monoanion of DHA and its derivatives. It follows that the cation interacts *via* the deprotonated carbon of the anions. The substituents at the deprotonated sites of $DMDHA^-$, $PDHA^-$ and $DPDHA^-$ hinder the cation's approach, encouraging cation solvation. Therefore, monolithium salts of these compounds exist mainly as SSIP in THF. The sodium, potassium and rubidium cations are less solvated than lithium and therefore their salts of $DMDHA^-$, $PDHA^-$ and $DPDHA^-$ exist as a mixture of CIP and SSIP.

Despite the presence of a substituent at the carbanion site, the monometallic salts of CNDHA exist as CIP in THF. The UV–VIS absorption shows a red shift with increasing cation size (Table 1). The rationale for this different behaviour is the existence of CIP of monometallic salts of CNDHA in which the cation is coordinated by a nitrogen atom of the CN group. According to calculations,[2] a considerable amount of the negative charge is concentrated on the nitrogen, so steric hindrance is not a significant factor. Shatenshtein[9] originally

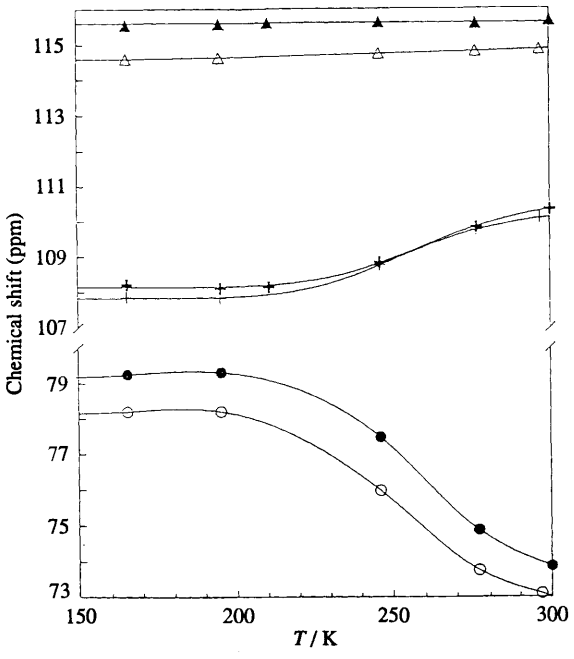

Fig. 1 Temperature dependences of the chemical shifts of C-2 (+, +), C-4 (△, ▲), and C-10 (○, ●) of sodium 9-methyl-9,10-dihydroanthracen-10-ide and sodium 9-phenyl-9,10-dihydroanthracen-10-ide: MDHA, empty symbols; PDHA, filled symbols

suggested such a mechanism of stabilization for cyano substituted anions.

Cation coordination

The size of the DHA anion (~ 8.5 Å) is significantly larger than an alkali-metal cation (up to 2 Å). The negative charge is concentrated on particular atoms of the anion, however, the cation is coordinated to one particular atom in CIP. The dipolar interaction at the coordination site displaces negative charge towards it, thus increasing the electronic shielding while electronic shielding of other carbon atoms decreases. As the temperature increases, the cation's solvent shell becomes thinner and the interionic distance decreases.[17] Therefore, the electronic shielding of this carbon atom increases, leading to an upfield shift in the ^{13}C NMR spectrum. On the other hand, the chemical shift of more distant carbons shifts downfield.

Fig. 1 shows the temperature dependences of the chemical shifts of C-2, C-4 and C-10 of MDHA-10$^-$Na$^+$ and PDHA-10$^-$Na$^+$. For each salt, the chemical shift of the deprotonated carbon atom decreases (shifts upfield) with temperature. However, the chemical shifts of other carbon atoms increase (shift downfield). The downfield chemical shift change is significantly larger in the *para* (to the coordination site) or *ortho* positions. The changes in other chemical shifts are negligible.

From these data and the above reasoning, it follows that monometallic salts of DHA and its derivatives coordinate *via* the deprotonated carbon. This is consistent with UV–VIS observations (*vide infra*).

Anion structure

The influence of anion structure on SSIP and CIP formation and stability was studied with reference to the proton chemical shifts' temperature dependence of monosodium salts of DHA and its derivatives (Figs. 2–9). For monometallic salts measurements were made in the concentration range 0.05–400 mmol dm^{-3}. Chemical shifts did not vary significantly with concentration changes of less than 5 mmol dm^{-3}. In all cases, the chemical shift variation with temperature and concentration was completely reversible.

Two types of monometallic salt were observed for

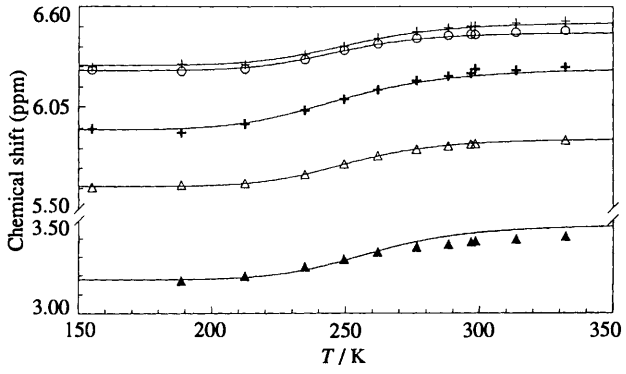

Fig. 2 Temperature dependence of proton chemical shift of sodium 9,10-dihydroanthracenide: +, 1-H; △, 2-H; ○, 3-H; +, 4-H; ▲, 9-H

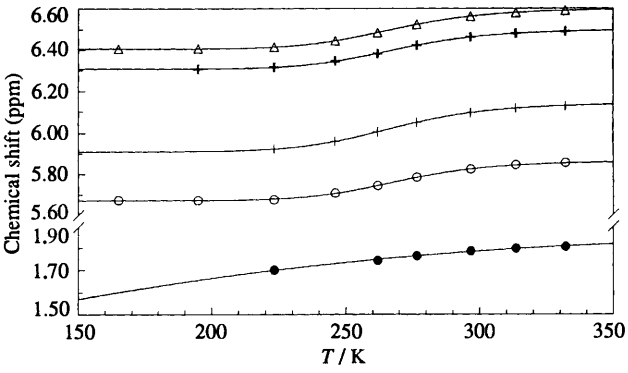

Fig. 3 Temperature dependence of proton chemical shift of sodium 9-methyl-9,10-dihydroanthracen-9-ide: +, 1-H; △, 2-H; ○, 3-H; +, 4-H; ●, 1′-H

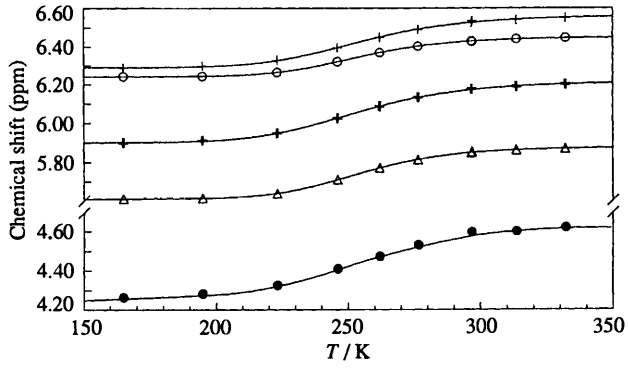

Fig. 4 Temperature dependence of proton chemical shift of sodium 9-methyl-9,10-dihydroanthracen-10-ide: +, 1-H; △, 2-H; ○, 3-H; +, 4-H; ●, 10-H

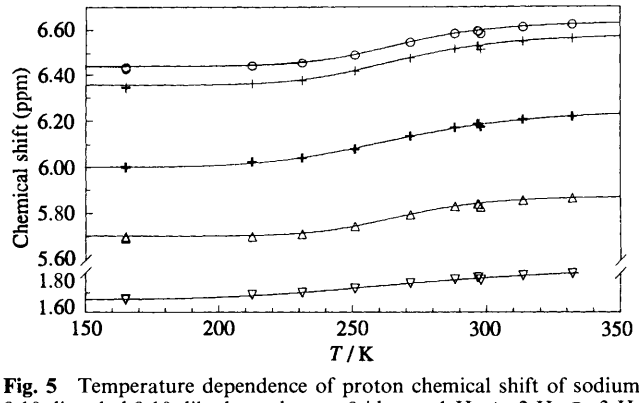

Fig. 5 Temperature dependence of proton chemical shift of sodium 9,10-dimethyl-9,10-dihydroanthracen-9-ide: +, 1-H; △, 2-H; ○, 3-H; +, 4-H; ▽, 1″-H

monosubstituted DHAs (MDHA and PDHA). Deprotonation at C-9 yields one salt and at C-10 yields the other.

Except for CNDHA-9$^-$Na$^+$, the temperature dependence of

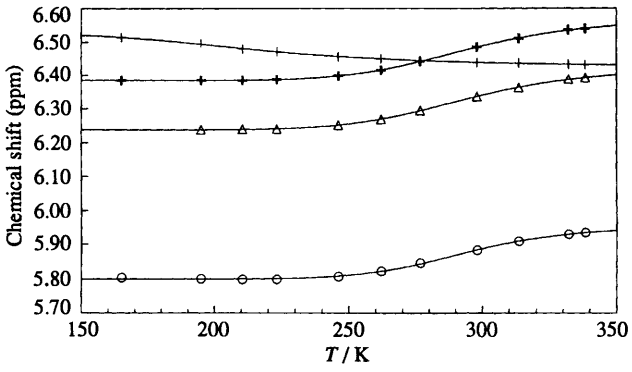

Fig. 6 Temperature dependence of proton chemical shift of sodium 9-phenyl-9,10-dihydroanthracen-9-ide: +, 1-H; △, 2-H; ○, 3-H; +, 4-H

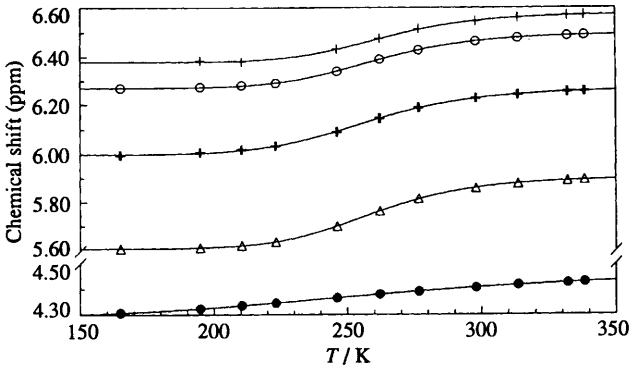

Fig. 7 Temperature dependence of proton chemical shift of sodium 9-phenyl-9,10-dihydroanthracen-10-ide: +, 1-H; △, 2-H; ○, 3-H; +, 4-H; ●, 10-H

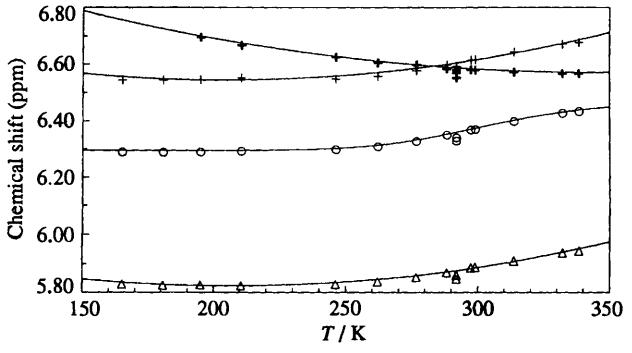

Fig. 8 Temperature dependence of proton chemical shift of sodium 9,10-diphenyl-9,10-dihydroanthracen-9-ide: +, 1-H; △, 2-H; ○, 3-H; +, 4-H

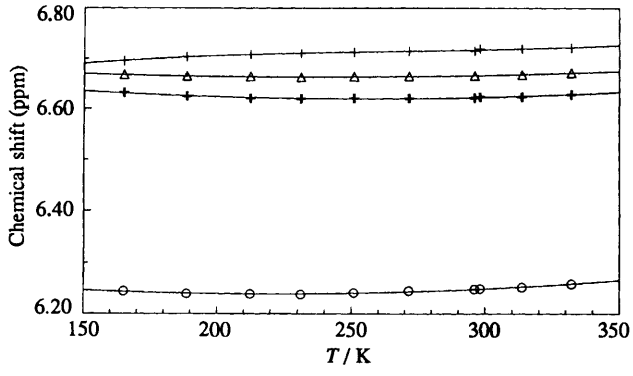

Fig. 9 Temperature dependence of proton chemical shift of sodium 9-cyano-9,10-dihydroanthracen-9-ide: +, 1-H; △, 2-H; ○, 3-H; +, 4-H

every anthracene proton chemical shift follows a sigmoid curve. Each anthracene proton of a given compound displays the same behaviour (Figs. 2–9). The proton signals shift downfield with increasing temperature.

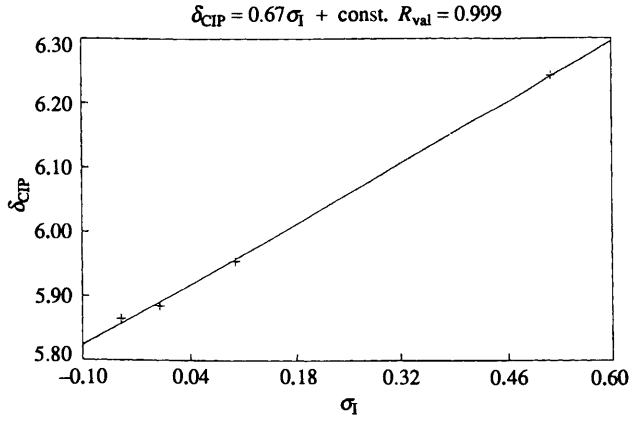

Fig. 10 Anionic stability as a function of substituent inductive effect

The proton chemical shift of the site of deprotonation showed the greatest sensitivity to electron density. However, we used the proton signals on the anthracene unit's outer rings and especially those *para* to the deprotonation site for our discussion. There are a number of reasons for this. Many anions (MDHA-9$^-$, PDHA-9$^-$, CNDHA-9$^-$, DMDHA$^-$ and DPDHA$^-$) have no proton at the deprotonated site. The *para* proton is the second most sensitive. Other protons are more subject to the influences of the cation field and the ring current and may not accurately reflect the charge distribution.[18]

Along with other data Table 2 contains *para* proton chemical shifts of SSIP and CIP, and CIP concentrations for monosodium salts of DHA and its derivatives (see the Discussion section).

The observed temperature dependences were interpreted in terms of solution equilibria between two ion pair types as described by Smid[15] and Szwarc.[17] At low temperature, the solvating THF molecules surround the cation in a large stable shell that hinders interionic contact. However, the ions are still connected electrostatically forming an SSIP. At higher temperatures, the molecular energy increases permitting the THF molecules to depart from the cation's solvent shell. Under these conditions, the ions are in direct contact forming CIP. The transition from SSIP to CIP changes the stabilization mechanism of the anion.

The major factor in CIP stabilization is interionic interaction. In CIP the cation is attracted to the anion by the electric field and the negative charge is withdrawn to the carbanion centre. Thus the electronic shielding of the other carbon and hydrogen atoms on the anthracene unit decreases. In SSIP, the interionic distance is large, consequently the cation's influence on the negative charge stabilization is weak. The stabilization of the negative charge in an SSIP anion occurs mainly *via* p–π conjugation of the deprotonated carbon atom's free pair with the π-electron system of the anthracene's outer rings. Therefore electron density is distributed to the outer rings and their SSIP proton chemical shifts are upfield of those of CIP.

The introduction of a substituent at the carbanion centre affects the anion stability of CIP and SSIP. For the series of SSIP states: DHA$^-$Na$^+$, MDHA-9$^-$Na$^+$ and PDHA-9$^-$Na$^+$, the *para* proton chemical shift increases in the order H < Me < Ph (Table 2). This observation shows that in SSIP, methyl and phenyl groups act as electron acceptors stabilizing the anion. In certain cases, the methyl group behaves as an electron acceptor and stabilizes the anion. Such behaviour of a methyl substituent is explained by hyperconjugation. For this effect to occur, a specific spatial orientation between the methyl substituent and the anion centre is required.[19,20] In SSIP the cation is distant from the anionic centre so the methyl can bend out of the anthracene plane to attain a favourable orientation for σ,π-conjugation (hyperconjugation).

For CIP, the signal of the *para* proton shifts downfield with

Table 2 Thermodynamic parameters ($\Delta H°$ and $\Delta S°$), equilibrium constants (K_{298}) for the transition from SSIP to CIP, *para* proton chemical shifts of CIP and SSIP of monometallic salts of DHA and its derivatives, proportion of CIP at 298 K ($[CIP]_{298}$) and net ($\sigma + \pi$)- and π-electron densities on the deprotonated carbon atoms[2]

Salt	$\Delta H°$/kcal mol^{-1}	$\Delta S°$/cal mol^{-1} K^{-1}	K_{298}	δ_{SSIP}	δ_{CIP}	$\delta_{CIP} - \delta_{SSIP}$	$[CIP]_{298}$ (%)	$(\pi + \sigma)$	π
DHA$^-$Li$^+$	6.3 ± 0.4	25.4 ± 1.5	8.8	5.615	5.885	0.270	90	−0.412	−0.369
MDHA-9$^-$Na$^+$	8.0 ± 0.2	29.7 ± 0.5	4.3	5.670	5.865	0.195	81	−0.368	−0.374
PDHA-9$^-$Na$^+$	7.7 ± 0.3	26.5 ± 1.1	1.4	5.798	5.955	0.157	58	−0.358	−0.413
CNDHA-9$^-$Na$^+$	—	—	∞	—	6.243	—	100	—	—
DMDHA$^-$Na$^+$	7.1 ± 0.7	27.1 ± 2.3	5.3	5.691	5.871	0.180	84	0.370	−0.372
DPDHA$^-$Na$^+$	8.5 ± 0.4	28.3 ± 1.2	0.9	5.826	5.966	0.140	47	−0.360	−0.410
MDHA-10$^-$Na$^+$	6.8 ± 0.4	27.1 ± 1.3	8.9	5.603	5.877	0.274	90	−0.412	−0.367
PDHA-10$^-$Na$^+$	6.9 ± 0.3	26.7 ± 1.2	6.1	5.605	5.902	0.297	86	−0.411	−0.367

substitution in the order Me < H < Ph < CN. The influence of these substituents on the anionic stability corresponds directly to the substituent's inductive effect (Fig. 10). The methyl group and anthracene unit are not in the same plane in CIP so there is no hyperconjugation with it. The methyl group is an electron donor, therefore, the *para* proton signal of MDHA-9$^-$Na$^+$ as CIP is upfield of that of DHA$^-$Na$^+$. The phenyl and cyano groups are electron acceptors. Hence, the *para* proton chemical shift of PDHA-9$^-$Na$^+$ and CNDHA-9$^-$Na$^+$ as CIP are downfield of that of DHA$^-$Na$^+$.

The substituent effect on CIP is weaker than that on SSIP. For MDHA-9$^-$Na$^+$, DHA$^-$Na$^+$ and PDHA-9$^-$Na$^+$ the maximum difference between *para* proton chemical shifts for CIP is 0.090 ppm and for SSIP it is 0.183 ppm (Table 2). That means that the cation suppresses the substituent effect for CIP.

The size of the substituent is very important for CIP stability. The proportion of CIP in DHA$^-$Na$^+$ (90% at 298 K) is slightly larger than that in MDHA-9$^-$Na$^+$ (81% at 298 K) because hydrogen is smaller than the methyl substituent. The phenyl group is considerably larger and decreases CIP stability more than the methyl. Hence, the proportion of CIP in PDHA-9$^-$Na$^+$ is 58% at 298 K (Table 2).

Calculation of enthalpies and entropies of solvation, chemical shift of SSIP and CIP

For the monoanions studied, SSIP are of lower energy than CIP. The two states yield significantly different chemical shifts for many of the ^{1}H and ^{13}C nuclei. The rate of exchange is much faster than the NMR timescale so the observed chemical shift represents an averaging between two states. This is one example of the general case where an averaged property can be observed for a first-order reaction [eqns. (4) and (5) where K_{eq} is

$$\text{SSIP} \rightleftharpoons \text{CIP} \tag{4}$$

$$K_{eq} = [\text{CIP}]/[\text{SSIP}] \tag{5}$$

the equilibrium constant]. Under such circumstances, the dependence of the observed property (in this case δ) on temperature (T) yields the enthalpy (ΔH) and entropy (ΔS) of the reaction.

The chemical shift of the mixture is the weighted average of the chemical shifts of each component [eqn. (6)]. Dividing the

$$\delta = ([\text{SSIP}]\delta_{SSIP} + [\text{CIP}]\delta_{CIP})/([\text{SSIP}] + [\text{CIP}]) \tag{6}$$

numerator and denominator of eqn. (6) by [SSIP] and combining with eqn. (5) yields eqn. (7). Eqn. (7) may be inverted to express the equilibrium constant K_{eq} as a function of chemical shift [eqn. (8)].

$$\delta = (\delta_{SSIP} + K_{eq}\delta_{CIP})/(1 + K_{eq}) \tag{7}$$

$$K_{eq} = (\delta_{SSIP} - \delta)/(\delta - \delta_{CIP}) \tag{8}$$

K_{eq} Is dependent upon the free energy ($\Delta G°$) of transition of SSIP to CIP according to eqn. (9).

$$\ln (K_{eq}) = -\Delta G°/RT \tag{9}$$

$\Delta G°$ Is connected with the enthalpy ($\Delta H°$) and entropy ($\Delta S°$) of the conversion of SSIP into CIP by eqn. (10).

$$\Delta G° = \Delta H° - T\Delta S° \tag{10}$$

The equilibrium constant is thus correlated with $\Delta H°$ and $\Delta S°$ by eqn. (11).

$$R \ln (K_{eq}) = \Delta S° - \Delta H°/T \tag{11}$$

Chemical shifts were measured over a range of temperatures. For each nucleus, there are four parameters that needed to be determined: δ_{CIP}, δ_{SSIP}, $\Delta H°$ and $\Delta S°$. As a first approximation, δ_{CIP} was taken to be the chemical shift at the highest temperature measured and δ_{SSIP} the chemical shift at the lowest temperature. A linear regression of $R \ln (K_{eq})$ against $1/T$ yields first approximations of $\Delta H°$ and $\Delta S°$ [eqns. (9)–(11)]. These were used to generate new values of δ_{SSIP} and δ_{CIP} based on the first and last points, respectively, [eqns. (12), (13)] where δ'_{CIP} and δ'_{SSIP} are the new values).[21,22]

$$\delta'_{CIP} = \delta_{CIP} + (\delta_{CIP} - \delta_{SSIP})/\exp[(T_{highest}\Delta S - \Delta H)/RT_{highest}] \tag{12}$$

$$\delta'_{SSIP} = \delta_{SSIP} + (\delta_{SSIP} - \delta_{CIP})/\exp[(T_{lowest}\Delta S - \Delta H)/RT_{lowest}] \tag{13}$$

The iteration was repeated until the change was insignificant, then the values were used as initial guesses for a non-linear iteration using the Levenberg–Marquardt method.[23] The final non-linear iteration produced more consistent results than the linear iteration. Greatest consistency was obtained from the protons of the outer anthracene rings [24,18] and we used these for our calculations. The reason for imperfections in the results is that other factors such as ring-current effects[24] and steric hindrance affect the chemical shifts. Using similar concentrations for all temperatures minimized concentration effects. For each result, an average was calculated weighted by the errors returned in the covariance matrix of the non-linear fit. The errors were calculated from the distribution of the results arising from different NMR signals. The non-linear fit was sensitive to inaccurate data, yielding relatively large error values if one chemical shift was wrong. Repeated thorough checking of the data was required to yield accurate and consistent results.

Thermodynamics of conversion of SSIP into CIP

The temperature interval commonly used in thermodynamics to characterize conversion between two states is the range between the 10th and 90th percentile, that is, between the temperature

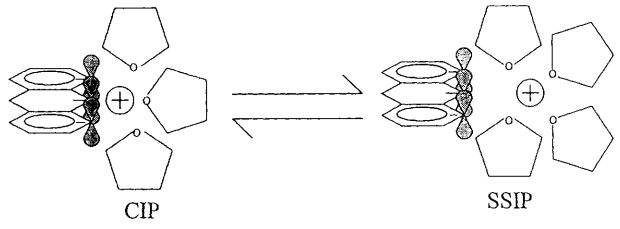

Fig. 11 Suggested model of conversion between CIP and SSIP: the solvent molecules are unable to squeeze between the cation and the anion due to steric hindrance

where the mixture is 90% SSIP and 10% CIP and that where the mixture is 10% SSIP and 90% CIP. For DHA^-Na^+, MDHA-10^-Na^+ and PDHA-10^-Na^+ the interval is 215–300 K. For MDHA-9^-Na^+ and $DMDHA^-Na^+$ the interval is somewhat narrower (230–300 K). For PDHA-9^-Na^+ and $DPDHA^-Na^+$ the interval is narrower still (255–300 K). Table 2 contains the values of the equilibrium constants (K_{eq}) at 298 K along with other thermodynamic parameters for the conversion of SSIP into CIP.

These thermodynamic terms were analysed according to published theories.[15,16] The theories may be summarized as follows. The driving force behind the conversion of CIP into SSIP is the energy of ion solvation for alkali-metal salts of DHA and its derivatives in THF. The entropy term (ΔS) depends on the change in the degree of freedom ('freezing out') of the solvent molecules as a consequence of their restricted position around the cation. In THF, where anion solvation is insignificant, the entropy term is practically independent of anion structure. Therefore, the entropy term for all the sodium salts studied was 27 ± 2 cal mol^{-1} K^{-1} (Table 2). Likewise, the entropies of conversion previously reported for the mono-sodium salts of fluorene,[18,25,26] triphenylmethane[18,25] and diphenylmethane[18] in THF are very similar to our results. The previously reported entropies were determined by UV–VIS, ^1H NMR and ^{13}C NMR spectroscopies while those determined by ^1H NMR spectroscopy[25] most closely corresponded to our results.

The enthalpy term (ΔH) consists of two opposing components. One is the energy of coulombic interaction between the cation and anion ($\Delta H_{coulomb}$). This component attracts the ions to each other and encourages the conversion of SSIP into CIP. The second component is the energy gain of cation solvation upon CIP to SSIP transition (ΔH_{sol}). This component promotes the conversion of CIP into SSIP. In THF, the conversion of CIP into SSIP is exothermic. Hence, the magnitude of ΔH_{sol} is larger than that of $\Delta H_{coulomb}$. It may be assumed that ΔH_{sol} does not vary for sodium salts of DHA and its derivatives because anion solvation is very weak. Therefore, the variation in the total enthalpy (ΔH) arises mainly from changes in the enthalpy of coulombic interaction. However, as $\Delta H \approx \Delta H_{sol} - \Delta H_{coulomb}$ and $|\Delta H_{sol}| > |\Delta H_{coulomb}|$, the variations of ΔH and $\Delta H_{coulomb}$ are in the opposite sense, *i.e.*, an increase in $\Delta H_{coulomb}$ leads to a decrease in ΔH.

In Table 2 the $\Delta H°$ values for the conversion of SSIP into CIP compare with total ($\sigma + \pi$)- and π-electron densities on the carbanion centres of monoanions of DHA and its derivatives. The anions studied can be divided into two groups according to the charge densities on their carbanion centres: DHA^-, MDHA-10^- and PDHA-10^- *versus* MDHA-9^-, $DMDHA^-$, PDHA-9^- and $DPDHA^-$. The same division can also be made using the $\Delta H°$ term. The $\Delta H_{coulomb}$ and total ($\sigma + \pi$) charge on the deprotonated carbon are greater in the former group than in the latter while the opposite is true for the π-electron density. Hence, $\Delta H_{coulomb}$ is governed by the cation's electrostatic interaction with the carbanion centre's total charge.

The geometric and electronic structural similarity between anions of DHA and diphenylmethane as well as PDHA and triphenylmethane has been reported.[2,5] This is the main reason for the similarities in the sodium salts of these compounds' $\Delta H°$ of SSIP to CIP conversion: 8.2 kcal mol^{-1} for triphenylmethane,[25] 7.7 kcal mol^{-1} for PDHA, 7.6 kcal mol^{-1} for diphenylmethane[25] and 6.3 kcal mol^{-1} for DHA. (The value of 11.7 kcal mol^{-1} reported[18] for sodium triphenylmethanide in THF is very high. It should be noted that the values of $\Delta H°$ and $\Delta S°$ reported there for other salts are larger than those found in other papers.[25,26])

Model for conversion of CIP into SSIP

At present the accepted model for conversion of CIP to SSIP is as follows.[15,17] At a sufficiently high temperature, the CIP ions are so close to each other that solvent molecules cannot squeeze between them. In CIP the ion pairs are held together mainly by coulombic attraction. However, in CIP there is a somewhat weaker contribution from covalent chemical bonding. As the temperature falls, solvation of the outer region of the cation increases resulting in the weakening of the cation–anion interaction. The interionic distance increases and solvent molecules squeeze between the cation and anion. The solvent molecules then completely surround the cation and there is no direct interionic contact. Electrostatic interaction solely holds the ion pair together. This is how ions become solvent separated. The existence of two types of ion pair is usually observed spectroscopically. In particular, the UV–VIS spectra of an organometallic compound display two absorption peaks; the shorter wavelength signal being typical of CIP and the longer SSIP. Temperature change causes one peak to increase and the other to decrease in height. Lithium salts of DHA and its derivatives behave in this manner. However, with other alkali metals, DHA and its derivatives behave differently. At room temperature, they display only one maximum at a frequency close to that expected for CIP which at low temperature shifts towards the absorption frequency of SSIP. This behaviour suggests a different model for the conversion of CIP into SSIP.

Sodium and other heavier alkali-metal salts of DHA and its derivatives exist as CIP at room temperature. As the temperature decreases, the solvation of the outer region of the cation increases. The cation–anion bond weakens and the interionic distance increases. However, because of the anion's structural properties and electronic structure, the solvent molecules cannot squeeze between the ions until the cation–anion bond length approaches the interionic distance required for SSIP.

Fig. 11 shows the structure of a CIP salt of DHA. In CIP, the cation is coordinated with the carbanion centre. THF molecules can solvate large cations only from behind because the anion's negatively charged *ortho* (to the carbanion centre) carbons block frontal approach.[2] In order for the THF molecules to enter, the interionic distance must be large. Therefore, for such salts, the transition from CIP to SSIP is gradual and the simultaneous existence of two types of ion pair is practically impossible. This effect arises because the DHA anion is rigid. The outer rings do not twist and so block frontal approach by solvent molecules (Fig. 10).

This model fits for ion pairs with large cations where the distance between the cation and the *ortho* carbons is small. In the case of lithium salts of DHA, frontal approach by the THF is possible and this salt exists as a mixture of CIP and SSIP.

Conclusions

The lithium salts of DHA and MDHA exist as a mixture of SSIP and CIP in THF at room temperature. Other alkali-metal salts of these compounds yield CIP under these conditions. Upon cooling, some CIP are converted into SSIP.

Alkali-metal salts of CNDHA exist exclusively as CIP.

Lithium salts of PDHA, DMDHA and DPDHA exist as SSIP at room temperature while salts of other alkali metals exist as mixtures of CIP and SSIP.

In general the cation in CIP is coordinated to the carbanion centre. Substituents at the carbanion centre hinder the formation of CIP. The stabilizing effect of the substituent is more significant for SSIP than for CIP.

The entropy of conversion of SSIP into CIP is governed by the change in the degree of freedom of the solvent molecules due to cation solvation. For the monosodium salts of DHA and its derivatives, the magnitude of $\Delta S°$ of transition is 27 ± 2 cal mol^{-1} K^{-1}. The enthalpy of conversion consists of two opposing components. One is the energy of coulombic interaction between the cation and anion and the other is the energy gain due to solvation. The enthalpy increases as the substituent size increases and as the negative charge on the deprotonated carbon atom decreases.

The high stability of CIP of DHA and its derivatives with sodium and heavier alkali metals is due to the unusual spatial structure and electron distribution of the anions. This prevents solvent molecules from squeezing between the cation and the anion.

Experimental

^1H and ^{13}C NMR spectra were recorded on a Bruker AMX-400 spectrometer for samples in [$^2H_8$]THF. As alkali-metal counter-anions react with tetramethylsilane (TMS), the chemical shifts were referenced to the most downfield solvent peaks, which are the best resolved signals of the solvent. The chemical shifts were determined from the multiplets' centres of gravity. The solvent chemical shifts were determined for pure [$^2H_8$]THF (99.65% atom D) containing TMS (< 5 mmol dm^{-3}). Varying the concentration of TMS up to 5 mmol dm^{-3} had no perceptible (< 0.001 ppm) effect on the chemical shift. The temperature was determined using a standard methanol NMR thermometer at temperatures up to 340 K and a standard ethylene glycol thermometer for higher temperatures.[27,28]

Melting points were determined on a Thomas–Hoover capillary melting point apparatus and are uncorrected.

Materials

Commercial samples of anthracene, 9,10-dihydroanthracene, 9-methylanthracene, 9,10-dimethylanthracene, 9-phenylanthracene, 9,10-diphenylanthracene and 9-cyanoathracene were purified by multiple recrystallization (methanol) and/or vacuum sublimation. Alkali metals were of commercial origin.

[$^2H_8$]THF

The commercial solvent was treated as previously reported.[1] The [$^2H_8$]THF was placed in a flask equipped with a vacuum line, then degassed in several freeze–pump–thaw cycles before being vacuum transferred into a flask containing distilled Na : K 5 : 1 alloy. This was then sonicated until a blue colour developed. The flask was allowed to stand overnight then sonicated again until a permanent blue colour developed. The solvent was then vacuum transferred to another flask containing distilled Na/K alloy.

Preparation of anions

Except for lithium salts, the alkali metal was distilled into the upper part of an extended NMR tube containing the anthracene derivative (~ 5 mg). Dry [$^2H_8$]THF was vacuum transferred into the tube, which was then sealed under vacuum.[1] Repeated inversion of the tube brought the solution into contact with the sodium. ^1H NMR spectroscopy detected the formation of the dianion. The monoanions were prepared in the same way, except that either a stoichiometric quantity of methanol was introduced with the anthracene derivative or the dihydroanthracene derivative was used.

Anthracene

Mp 217–218 °C (lit.,[29,30] 216–218 °C); δ_H([$^2H_8$]THF; 295 K) 7.42 (2-H) and 8.00 (1-H) (AA′XX′, each 4 H) and 8.44 (s, 2 H, 9-H); δ_C([$^2H_8$]THF; 295 K) 126.07 (d, $^1J_{CH}$ 159.8, C-2), 126.92 (d, $^1J_{CH}$ 156.9, C-9), 128.93 (d, $^1J_{CH}$ 161.1, C-1) and 132.83 (s, C-4a).

9,10-Dihydroanthracene

Mp 108–109 °C (lit.,[31] 108–110 °C); δ_H([$^2H_8$]THF; 295 K) 3.90 (s, 4 H, 9-H) and 7.12 (2-H) and 7.25 (1-H) (AA′XX′, each 4 H); δ_C([$^2H_8$]THF; 295 K) 36.72 (t, $^1J_{CH}$ 127.0, C-9), 126.71 (d, $^1J_{CH}$ 159.3, C-1), 126.98 (d, $^1J_{CH}$ 155.6, C-2) and 137.72 (s, C-4a).

9-Methylanthracene

Mp 81–82 °C (lit.,[32] 81.5 °C); δ_H([$^2H_8$]THF; 297.0 K) 3.08 (s, 3 H, 1′-H), 7.42 (t, 2 H, 3-H), 7.47 (t, 2 H, 2-H), 7.99 (d, 2 H, 4-H), 8.30 (d, 2 H, 1-H) and 8.35 (s, 1 H, 10-H); δ_C([$^2H_8$]THF; 297.0 K; 34 mmol dm^{-3}) 23.59 (C-1′), 125.39 (C-1), 125.50 (C-3), 125.97 (C-2), 126.12 (C-10), 127.99 (C-9), 129.81 (C-4), 131.18 (C-8a) and 132.65 (C-4a).

9-Cyanoanthracene

Mp 175–177 °C (lit.,[33] 173–177 °C); δ_H([$^2H_8$]THF; 296.8 K) 7.60 (t, 2 H, 3-H), 7.75 (t, 2 H, 2-H), 8.16 (d, 2 H, 4-H), 8.38 (d, 2 H, 1-H) and 8.84 (s, 1 H, 10-H); δ_C([$^2H_8$]THF; 296.8 K) 106.40 (C-1′), 117.22 (C-9), 125.80 (C-1), 127.24 (C-3), 129.96 (C-2), 130.02 (C-4), 131.83 (C-4a), 133.72 (C-10) and 134.08 (C-8a).

9-Phenylanthracene

Mp 154–155 °C (lit.,[34] 153–155 °C); δ_H([$^2H_8$]THF; 295 K) 7.31 (t, 2 H, 2-H), 7.40 (d, 2 H, 2′-H), 7.43 (t, 2 H, 3-H), 7.52 (t, 1 H, 4′-H), 7.57 (t, 2 H, 3′-H), 7.61 (d, 2 H, 1-H), 8.05 (d, 2 H, 4-H) and 8.53 (s, 1 H, 10-H); δ_C([$^2H_8$]THF; 295 K) 125.81 (C-3), 126.09 (C-2), 127.39 (C-10), 127.43 (C-1), 128.28 (C-4′), 129.16 (C-4), 129.22 (C-3′), 131.18 (C-8a), 132.05 (C-2′), 132.54 (C-4a), 137.81 (C-1′) and 139.90 (C-9).

9,10-Dimethylanthracene

Mp 179–181 °C (lit.,[35] 180–181 °C); δ_H([$^2H_8$]THF; 297.0 K; 18.6 mmol dm^{-3}) 3.08 (s, 3 H, 1′-H) and 7.47 (2-H) and 8.34 (1-H) (AA′XX′ each 4 H); δ_C([$^2H_8$]THF; 295.0 K) 23.41 (C-1′), 125.42 (C-2), 126.03 (C-1), 128.90 (C-9) and 130.96 (C-4a).

9,10-Diphenylanthracene

Mp 246–248 °C (lit.,[36] 245–248 °C); δ_H([$^2H_8$]THF; 295 K) 7.30 (2-H) and 7.65 (1-H) (AA′XX′, each 4 H), 7.45 (d, 4 H, 2′-H), 7.54 (t, 1 H, 4′-H) and 7.61 (t, 2 H, 3′-H); δ_C([$^2H_8$]THF; 295.0 K) 125.58 (C-2), 127.63 (C-1), 128.33 (C-4′), 129.07 (C-3′), 130.85 (C-4a), 132.10 (C-2′), 138.00 (C-1′) and 140.16 (C-9).

Sodium 9,10-dihydroanthracenide

δ_H([$^2H_8$]THF; 295 K) 3.04 (s, 1 H, 9-H), 4.30 (s, 2 H, 10-H), 5.86 (t, 2 H, 2-H), 6.30 (d, 2 H, 4-H), 6.50 (t, 2 H, 3-H) and 6.53 (d, 2 H, 1-H); δ_C([$^2H_8$]THF; 295 K) 39.87 (t, $^1J_{CH}$ 123.1, C-9), 72.23 (d, $^1J_{CH}$ 146.7, C-10), 110.68 (d, $^1J_{CH}$ 157.8, C-2), 114.73 (d, $^1J_{CH}$ 149.8, C-4), 120.48 (s, C-8a), 126.35 (d, $^1J_{CH}$ 150.2, C-3), 126.69 (d, $^1J_{CH}$ 149.5, C-1) and 146.44 (s, C-4a).

Sodium 9-methyl-9,10-dihydroanthracen-9-ide

δ_H([$^2H_8$]THF; 295 K) 1.78 (s, 3 H, 1′-H), 3.47 (s, 2 H, 10-H), 5.82 (t, 2 H, 3-H), 6.01 (d, 2 H, 1-H), 6.56 (t, 2 H, 2-H) and 6.46 (d, 2 H, 4-H); δ_C(partial spectrum; [$^2H_8$]THF; 295 K) 43.89 (C-10), 108.3 (C-3), 110.33 (C-1), 126.48 (C-2) and 125.55 (C-4).

Sodium 9-methyl-9,10-dihydroanthracen-10-ide

δ_H([$^2H_8$]THF; 295 K) 1.00 (d, 3 H, 1′-H), 3.79 (q, 1 H, 9-H), 5.51 (s, 1 H, 10-H), 5.84 (t, 2 H, 2-H), 6.17 (d, 2 H, 4-H), 6.43 (t, 2 H, 3-H) and 6.52 (d, 2 H, 1-H); δ_C([$^2H_8$]THF; 295 K) 24.88 (C-1′), 43.4 (C-9), 73.00 (C-10), 107.84 (C-2), 114.85 (C-4), 124.94 (C-8a), 126.32 (C-3), 127.15 (C-1) and 142.98 (C-4a).

Sodium 9-cyano-9,10-dihydroanthracen-9-ide
δ_H([$^2H_8$]THF; 295 K) 3.87 (s, 2 H, 10-H), 6.25 (t, 2 H, 3-H), 6.62 (d, 2 H, 4-H), 6.67 (t, 2 H, 2-H) and 6.61 (d, 2 H, 1-H); δ_C([$^2H_8$]THF, 295 K) 37.69 (C-10), 55.89 (C-9), 115.96 (C-3), 117.92 (C-1), 125.00 (C-4a), 125.90 (C-2), 127.07 (C-4), 135.09 (C-1′) and 142.49 (C-8a).

Sodium 9-phenyl-9,10-dihydroanthracen-9-ide
δ_H([$^2H_8$]THF; 295 K) 3.68 (s, 2 H, 10-H), 5.80 (t, 2 H, 3-H), 6.24 (t, 2 H, 2-H), 6.44 (d, 2 H, 1-H), 6.48 (d, 2 H, 4-H), 6.75 (t, 1 H, 4′-H), 7.11 (t, 2 H, 3′-H) and 7.31 (d, 2 H, 2′-H); δ_C([$^2H_8$]THF; 295 K) 40.61 (C-10), 90.90 (C-9), 110.70 (C-3), 112.19 (C-1), 121.00 (C-4′), 121.46 (C-8a), 125.72 (C-2), 126.43 (C-4), 128.76 (C-3′), 133.23 (C-2′), 142.54 (C-4a) and 147.40 (C-1′).

Sodium 9-phenyl-9,10-dihydroanthracen-10-ide
δ_H([$^2H_8$]THF; 295 K) 4.40 (s, 1 H, 10-H), 4.87 (s, 1 H, 9-H), 5.85 (t, 2 H, 2-H), 6.22 (d, 2 H, 4-H), 6.46 (t, 2 H, 3-H), 6.54 (d, 2 H, 1-H), 6.90 (t, 1 H, 4′-H), 7.01 (t, 2 H, 3′-H) and 7.17 (d, 2 H, 2′-H); δ_C([$^2H_8$]THF; 295 K) 53.98 (C-9), 74.0 (C-10), 110.25 (C-2), 115.61 (C-4), 122.79 (C-4a), 125.23 (C-4′), 126.41 (C-3), 127.99 (C-3′), 128.28 (C-2′), 128.74 (C-1), 143.79 (C-8a) and 149.90 (C-1′).

Sodium 9,10-dimethyl-9,10-dihydroanthracenide
δ_H([$^2H_8$]THF; 295 K) 0.93 (d, 3 H, 1′-H), 1.78 (s, 3 H, 1″-H), 3.55 (q, 1 H, 9-H), 5.84 (t, 2 H, 2-H), 6.19 (d, 2 H, 4-H), 6.53 (d, 2 H, 1-H) and 6.59 (t, 2 H, 3-H); δ_C([$^2H_8$]THF; 295 K) 13.38 (C-1″), 24.31 (C-1′), 44.15 (C-9), 76.70 (C-10), 108.31 (C-2), 110.94 (C-4), 126.09 (C-1), 126.37 (C-8a), 126.38 (C-3) and 139.69 (C-4a).

Sodium 9,10-diphenyl-9,10-dihydroanthracenide
δ_H([$^2H_8$]THF; 295 K) 4.85 (s, 1 H, 9-H), 5.87 (t, 2 H, 2-H), 6.36 (t, 2 H, 3-H), 6.59 (d, 2 H, 4-H), 6.61 (d, 2 H, 1-H), 6.76 (t, 1 H, 4″-H), 6.85 (t, 1 H, 4′-H), 6.97 (t, 2 H, 3′-H), 7.08 (t, 2 H, 3″-H), 7.27 (d, 2 H, 2′-H) and 7.30 (d, 2 H, 2″-H); δ_C([$^2H_8$]THF; 295 K) 54.81 (C-9), 90.85 (C-10), 110.48 (C-2), 113.52 (C-4), 121.23 (C-4″), 123.55 (C-8a), 124.96 (C-4′), 125.60 (C-3), 127.70 (C-3′), 127.83 (C-2′), 128.44 (C-1), 128.56 (C-3″), 133.70 (C-2″), 140.35 (C-1′), 147.32 (C-1″) and 150.84 (C-4a).

Acknowledgements

We thank the US–Israel binational science foundation for financial support and the Margaret Thatcher Center of Interdepartmental Scientific Equipment for NMR facilities.

References

1 I. O. Shapiro, M. Nir, R. E. Hoffman and M. Rabinovitz, *J. Chem. Soc., Perkin Trans. 2*, 1994, 1519.
2 M. Nir, R. E. Hoffman, I. O. Shapiro and M. Rabinovitz, *J. Chem. Soc., Perkin Trans. 2*, 1995, 1433.
3 D. Nicholls and M. Szwarc, *J. Am. Chem. Soc.*, 1966, **88**, 5757.
4 D. Nicholls and M. Szwarc, *Proc. R. Soc. A*, 1967, **301**, 223.
5 D. Nicholls and M. Szwarc, *Proc. R. Soc. A*, 1967, **301**, 231.
6 M. Daney, H. Bouas-Laurent, B. Calas, L. Gizal and N. Platzer, *J. Organomet. Chem.*, 1987, **52**, 3521.
7 A. Sygula and P. W. Rabideau, *J. Org. Chem.*, 1987, **52**, 3521.
8 P. W. Rabideau, *Tetrahedron*, 1989, **45**, 1579.
9 T. I. Lebedeva, E. S. Petrov and A. I. Shatenshtein, *Russ. J. Org. Chem.*, 1977, **13**, 825.
10 A. Streiwieser, J. R. Murdoch, G. Hafelinger and C. J. Chang, *J. Am. Chem. Soc.*, 1973, **95**, 4248.
11 K. Müllen, W. Huber, G. Neumann, C. Schnieders and M. Unterberg, *J. Am. Chem. Soc.*, 1985, **107**, 801.
12 P. W. Rabideau, A. J. Maxwell and A. Sygula, *J. Org. Chem.*, 1986, **51**, 3181.
13 I. I. Bilkis, T. A. Vaganova, E. V. Pantaleeva, G. E. Salnikov, A. P. Tananakin, V. I. Mamatyuk and V. D. Shteingarts, *J. Phys. Org. Chem.*, 1994, **7**, 153.
14 P. Chang, R. V. Seates and M. Szwarc, *J. Phys. Chem.*, 1966, **70**, 3180.
15 J. Smid, in *Ions and Ion Pairs in Organic Reactions*, ed. M. Szwarc, Wiley–Interscience, New York, 1972, vol. 1, ch. 3.
16 E. Buncel and B. Menon, in *Comprehensive Carbanion Chemistry*, eds. E. Buncel and E. Durst, Elsevier, New York, Part A, ch. 3, 1980.
17 M. Szwarc, in *Ions and Ion Pairs in Organic Reactions*, ed. M. Szwarc, Wiley–Interscience, New York, 1972, vol. 1, ch. 1.
18 D. H. O'Brien, C. R. Russell and A. J. Hart, *J. Am. Chem. Soc.*, 1979, **101**, 633.
19 M. J. S. Dewar, *Hyperconjugation*, Ronald Press, New York, 1962.
20 P. R. Schleyer and A. J. Kos, *Tetrahedron*, 1983, **39**, 1141.
21 J. Rosengaus, *Ph.D Thesis*, The Hebrew University of Jerusalem, 1994.
22 I. Willner, J. Rosengaus and Y. Eichen, *J. Phys. Org. Chem.*, 1993, **6**, 29.
23 W. H. Press, B. P. Flannery, S. A. Teukolsky and W. T. Vetterling, *Numerical Recipes in C*, Cambridge University Press, Cambridge, UK, 1989.
24 D. H. O'Brien, C. R. Russell and A. J. Hart, *J. Am. Chem. Soc.*, 1976, **98**, 7427.
25 J. B. Grutzner, J. M. Lawlor and L. M. Jackman, *J. Am. Chem. Soc.*, 1972, **94**, 2306.
26 T. E. Hogen-Esch and J. Smid, *J. Am. Chem. Soc.*, 1966, **88**, 307.
27 A. L. Van Geet, *Anal. Chem.*, 1968, **40**, 2227.
28 A. L. Van Geet, *Anal. Chem.*, 1970, **42**, 679.
29 G. M. Badger, *J. Chem. Soc.*, 1952, 1175.
30 V. Gold and F. L. Tye, *J. Chem. Soc.*, 1952, 2172.
31 W. E. Parham, L. D. Jones and Y. A. Sayed, *J. Org. Chem.*, 1976, **41**, 1184.
32 A. Seiglitz and R. Marx, *Ber. Dtsch. Chem. Ges.*, 1923, **56**, 1619.
33 A. Mielert, C. Braig, J. Sauer, J. Martelli and R. Sustmann, *Liebigs Ann. Chem.*, 1980, 954.
34 E. Clar and D. Stewart, *J. Am. Chem. Soc.*, 1952, **74**, 6235.
35 C. S. Gibson and J. D. A. Johnson, *J. Chem. Soc.*, 1931, 753.
36 Y. Hirshberg, *Trans. Faraday Soc.*, 1948, **44**, 285.

Paper 5/04164C
Received 28*th June* 1995
Accepted 20*th November* 1995